Supplement of The Cryosphere, 19, 753–767, 2025
https://doi.org/10.5194/tc-19-753-2025-supplement

The Cryosphere
Open Access

Supplement of

Reconstructed glacier area and volume changes in the European Alps since the Little Ice Age

Johannes Reinthaler and Frank Paul

Correspondence to: Johannes Reinthaler (johannes.reinthaler@geo.uzh.ch)

S1 Supplementary tables

Table S1: List of historical maps with glacier extents available for the different Alpine countries.

County	Name	Date	Scale	Link
Switzerland	Dufour map	1845-1865	1:100000	https://www.swisstopo.admin.ch/en/geodata/maps/historical/dufour.html
	Siegfried map	1870-1926	1:50000	https://www.swisstopo.admin.ch/en/geodata/maps/historical/siegfried25.html
France	Carte de l'état major	1820-1866	1:40000	https://www.geoportail.gouv.fr/donnees/carte-de-letat-major-1820-1866
Italy	Übersichtskarte der Dolomiten	1903	1:100000	https://www.e-rara.ch/zut/content/titleinfo/29139322
	Austro-Hungarian Monarchy. Militärgeographisches Institut, Zone 19 col 6 (Toblach & Cortina d' Ampezzo)	1889	1:75000	https://digitalcollections.nypl.org/items/510d47df-8b8d-a3d9-e040-e00a18064a99
	Austro-Hungarian Monarchy. Militärgeographisches Institut, Zone 20 col 5 (Bozen & Fleimstal)	1882	1:75000	https://digitalcollections.nypl.org/items/510d47df-8bae-a3d9-e040-e00a18064a99
	Austro-Hungarian Monarchy. Militärgeographisches Institut, Zone 20 col 6 (Pieve Di Livinallongo und Longarone)	1882	1:75000	https://digitalcollections.nypl.org/items/510d47df-8bb0-a3d9-e040-e00a18064a99
Germany	Topographische Karte von Bayern 869, Hochkarlter 888, Zugspitze 870/871, St Bartholomä	1889-1897	1:25000	https://www.geodaten.bayern.de/histTopoKarten/01_Positionsblatt/01_869_F_1923.pdf https://www.geodaten.bayern.de/histTopoKarten/01_Positionsblatt/01_888_F_1936.pdf https://www.geodaten.bayern.de/histTopoKarten/01_Positionsblatt/01_870_F_1937.pdf
Slovenia	Studi Alpini fatti nella valle della Raccolana - Giacomo Savorgnan di Brazzà	1881	1:32000	https://www.abebooks.it/STUDI-ALPINI-FATTI-VALLE-RACCOLANA-Alpi/22916664602/bd

Table S2: Existing glacier outlines used for this study and their sources.

Country	Name, Reference	Date	Nr. glaciers	Mapping approach	Data Access
All	RGI 7.0, (RGI Consortium, 2023)	2003	4034	Satellite image mapping	Open access
	(Paul et al., 2020)	2015	4395	Sentinel-2	Open access
Switzerland	(Maisch et al., 2000)	LIA	2380	Digitisation of Siegfried map	GLIMS
	(Müller et al., 1976)	1973	2061	Areal photographs	glamos.ch
Austria	(Fischer et al., 2015)	LIA	645	Update of existing inventory using lidar and orthophotos	GLIMS
	(Groß, 1987)	1969	869		GLIMS
France	(Gardent, 2014)	LIA	694	Digitisation using maps, photographs and field investigation	Dataset shared by the author
	(Vivian, 1975)	1967-71	502		GLIMS
Italy (Aosta)	GlaRiskAlp	LIA	210		Open access dataset
Italy (Piemonte)	(Lucchesi et al., 2014)	LIA	96		Open access dataset
Italy (Lombardy)	(Scotti and Brardinoni, 2018)	LIA	11	Field-based and remotely-sensed mapping	Dataset shared by the author
Italy (Trentino)	(Zanoner et al., 2017)	LIA	159	Mapping using Lidar and high res. orthophotos	Dataset shared by the author
Italy (South Tyrol)	(Knoll et al., 2009)	LIA	300	Digitisation using high res. DEM, orthophotos and historic maps	Dataset shared by the author
Italy (Friuli) and Slovenia	(Colucci and Žebre, 2016)	LIA	20		Dataset shared by the author

Table S3: Previously missing glaciers and glaciers with new LIA outlines.

Region ID	Region name	Nr. of previously missing glacier (rgi v7.0)	Area (rgi v7.0) km^2 of previously missing glacier	Glacier count (rgi v7) with new LIA outlines	Area (rgi v7.0) with new LIA outlines	Glacier count with no LIA outline	Area (rgi v7.0) with no LIA outlines
1	Dauphiné Alps	54	10.04	27	9.23	27	0.81
2	Cottian & Maritime Alps	10	0.30	1	0.06	9	0.23
3	Graian Alps	28	1.26	1	0.23	27	1.03
4	Savoy Prealps	18	3.17	11	2.95	7	0.23
5	Pennine Alps	25	7.90	14	7.47	11	0.43
6	Bernese Alps	11	0.18	0	0.00	11	0.18
7	Glarus Alps	3	0.11	0	0.00	3	0.11
8	Lepontine Alps	38	2.35	16	1.84	22	0.51
9	Rhaetian Alps West	158	22.36	62	19.42	96	2.93
10	Rhaetian Alps East	2	0.03	0	0.00	2	0.03
11	Rhaetian Alps South	65	13.61	49	13.05	16	0.56
12	Tauern Alps West	15	2.21	7	2.03	8	0.18
13	Dolomites & Carnic Alps	33	2.33	22	1.94	11	0.39
14	Northeastern Alps	11	0.91	8	0.81	3	0.10
Total		471	66.77	218	59.04	253	7.73

Table S4: Glacier area, volume and change values per country. Data for P2 are from Hugonnet et al. (2021).

Country	Area LIA (km^2)	Area 2015 (km^2)	Relative area change P3 (%)	Volume LIA (km^3)	Volume 2015 (km^3)	Relative volume change (%)	Mean elevation change (P3) (m)	Increase in volume change rate (%) (P2 vs. P1)
France	569.28	225.63	-60.37	34.24	12.21	-64.33	-41.44	35.59
Switzerland	1789.02	889.88	-50.26	132.21	59.33	-55.12	-41.41	24.89
Italy	970.62	318.59	-67.18	57.67	14.76	-74.41	-45.36	39.04
Austria	910.97	358.27	-60.67	55.36	13.32	-75.94	-47.68	37.21
Germany	3.74	0.30	-91.98	0.14	0.003	-97.81	-37.91	61.24
Slovenia	0.82		-100.00	0.01		-100.00	-21.45	

Table S5: Glacier area, volume and change values per basin. The basins of the Adige, Brenta, Piave, Tagliamento and Soča are listed together under south-eastern Alps. Data for P2 from Hugonnet et al. (2021).

Basin	Area LIA (km^2)	Area 2015 (km^2)	Relative area change P3 (%)	Volume LIA (km^3)	Volume 2015 (km^3)	Volume change rate P1 (km^3 a^{-1})	Volume change rate P2 (km^3 a^{-1})	Increase in volume change rate (%) (P2 vs. P1)
Rhône	1513.48	781.47	-48.37	116.63	53.48	-0.38	-0.78	57.56
south-eastern Alps	345.73	92.01	-73.39	18.55	3.11	-0.09	-0.08	-13.49
Po	727.35	269.80	-62.91	44.33	13.06	-0.19	-0.23	25.15
Danube	1026.92	397.32	-61.31	60.74	15.13	-0.28	-0.30	12.86
Rhine	630.96	265.29	-57.95	39.38	14.85	-0.15	-0.29	56.97

S2 Supplementary figures

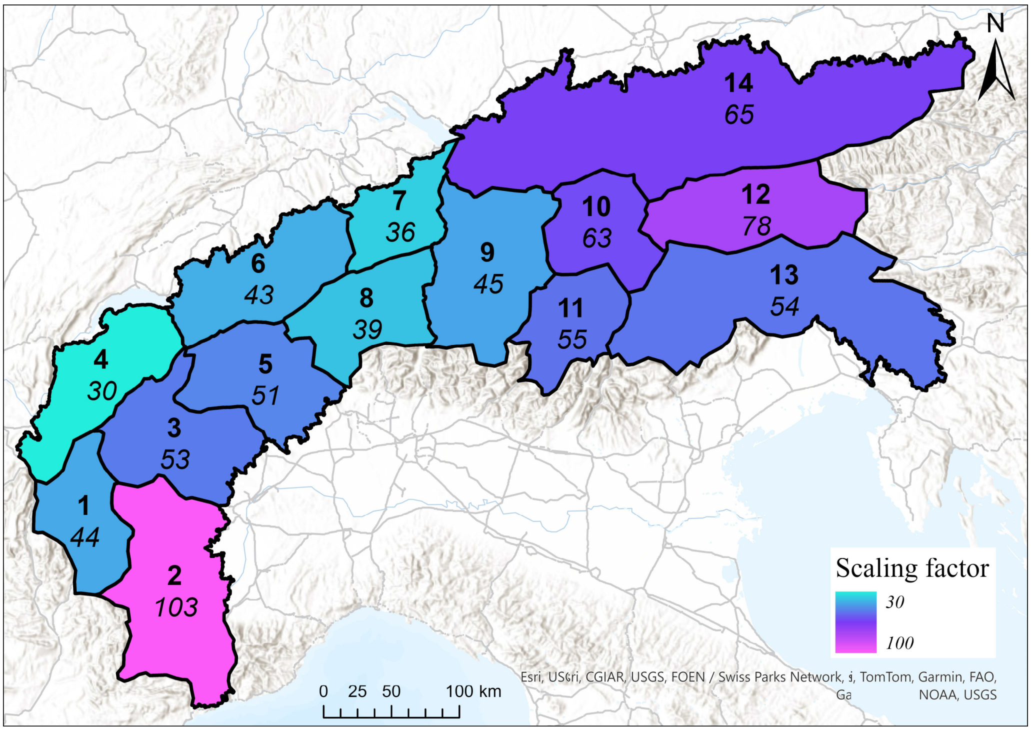

Figure S1: Region IDs (bold) and scaling factors (italic) used for the LIA surface reconstruction.

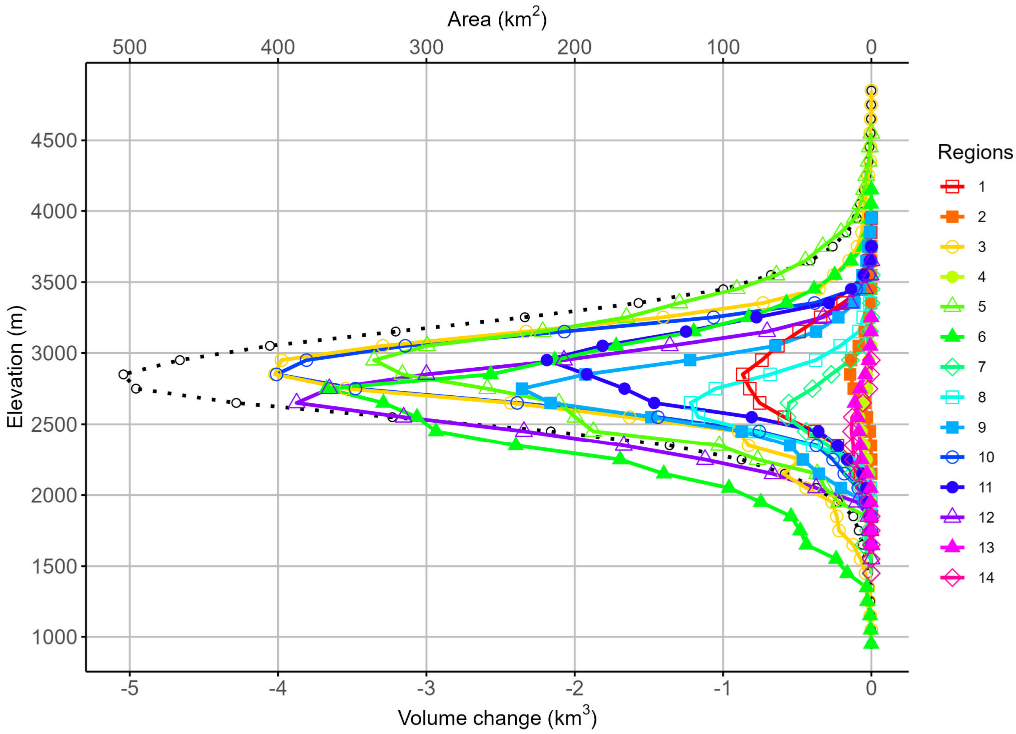

Figure S2: Volume change (P3) for the 14 subregions (the black dotted line indicates the area in the specific elevation).

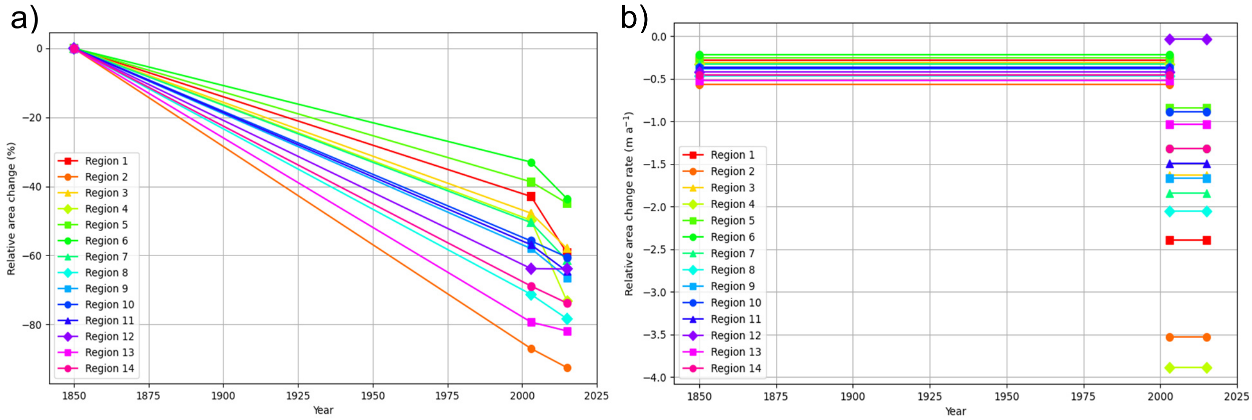

Figure S3: a) Relative glacier area change per region. b) relative area change rate per region.

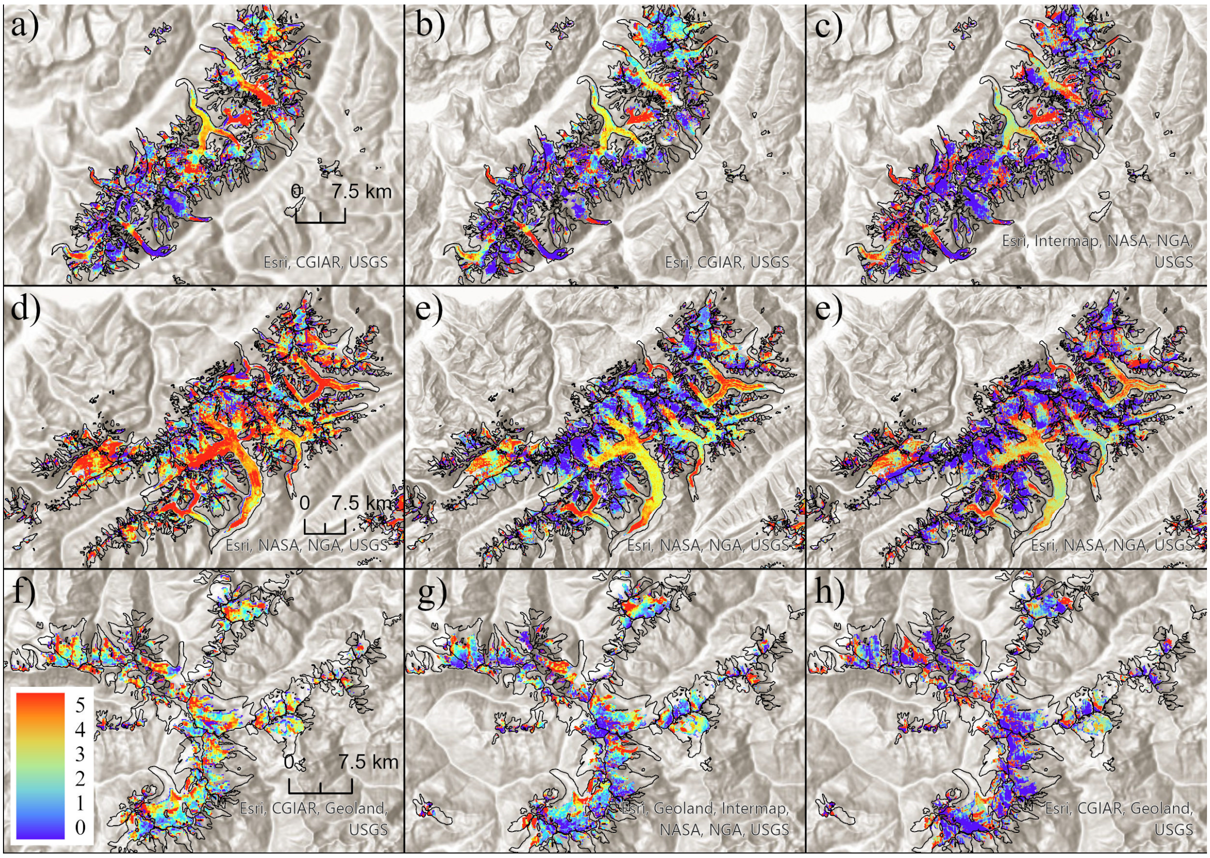

Figure S4: Acceleration rate after 2000 calculated for a), d), f) from Hugonnet et al. (2021), b), e), g) from Sommer et al. (2020) and c), e), h) from the difference of the SRTM DEM and the Copernicus DEM. The acceleration rate is shown as a dimensionless factor, representing the relative increase (e.g., 3 = threefold increase). The mountain ranges are a-c) Mt. Blanc, d-e) Bernese Alps, f-h) Ortles range. All background images: ESRI, (2023a).

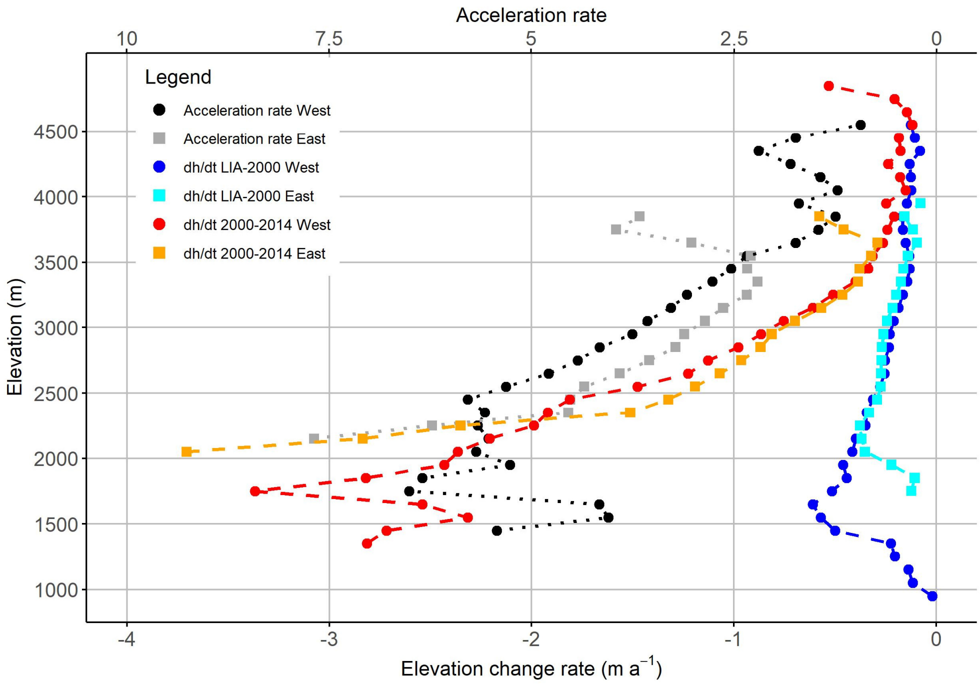

Figure S5: Elevation change rates LIA to 2000 (P1) and 2000 to 2014 (P2) from Hugonnet et al. (2021) as well as the acceleration rate for the eastern and western Alps.

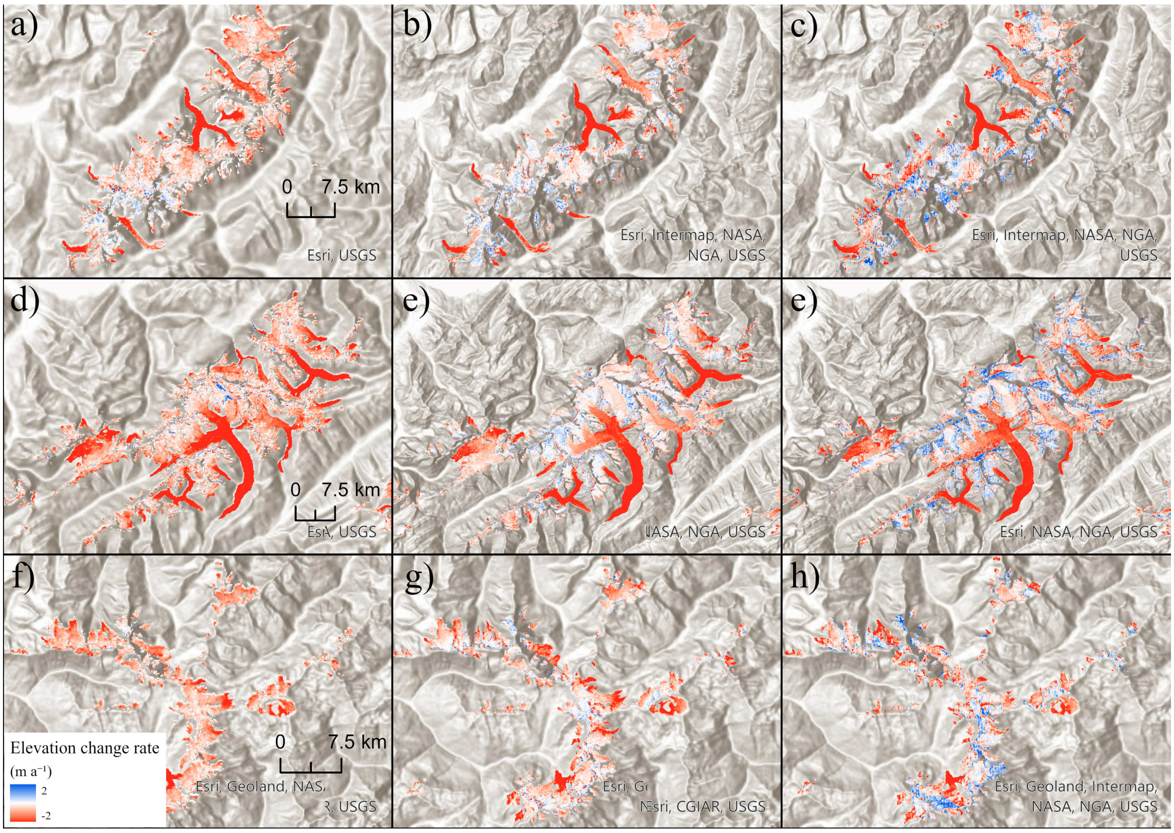

Figure S6: Elevation change rate (m) for P2 a), d), f) from Hugonnet et al. (2021), b), e), g) from Sommer et al. (2020) and c), e), h) from the difference of the SRTM DEM and the COP DEM. The mountain ranges are a-c) Mt. Blanc, d-e) Bernese Alps, f-h) Ortles range. All background images: ESRI, (2023a).

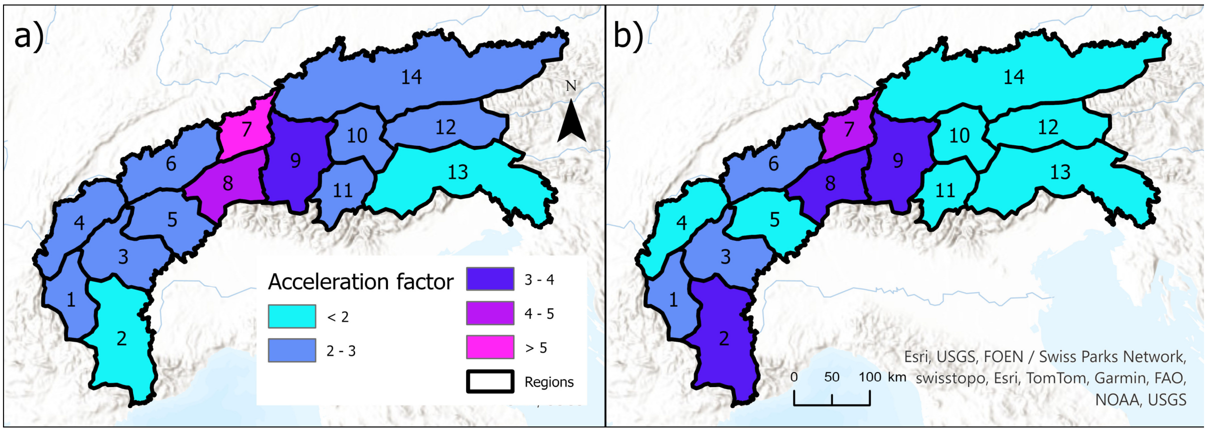

Figure S7: Acceleration factor from comparing elevation change rates of a) LIA to SRTM to Sommer et al. (2020) and b) LIA to SRTM compared to the SRTM to COP DEM period. All background images: ESRI, (2023a).

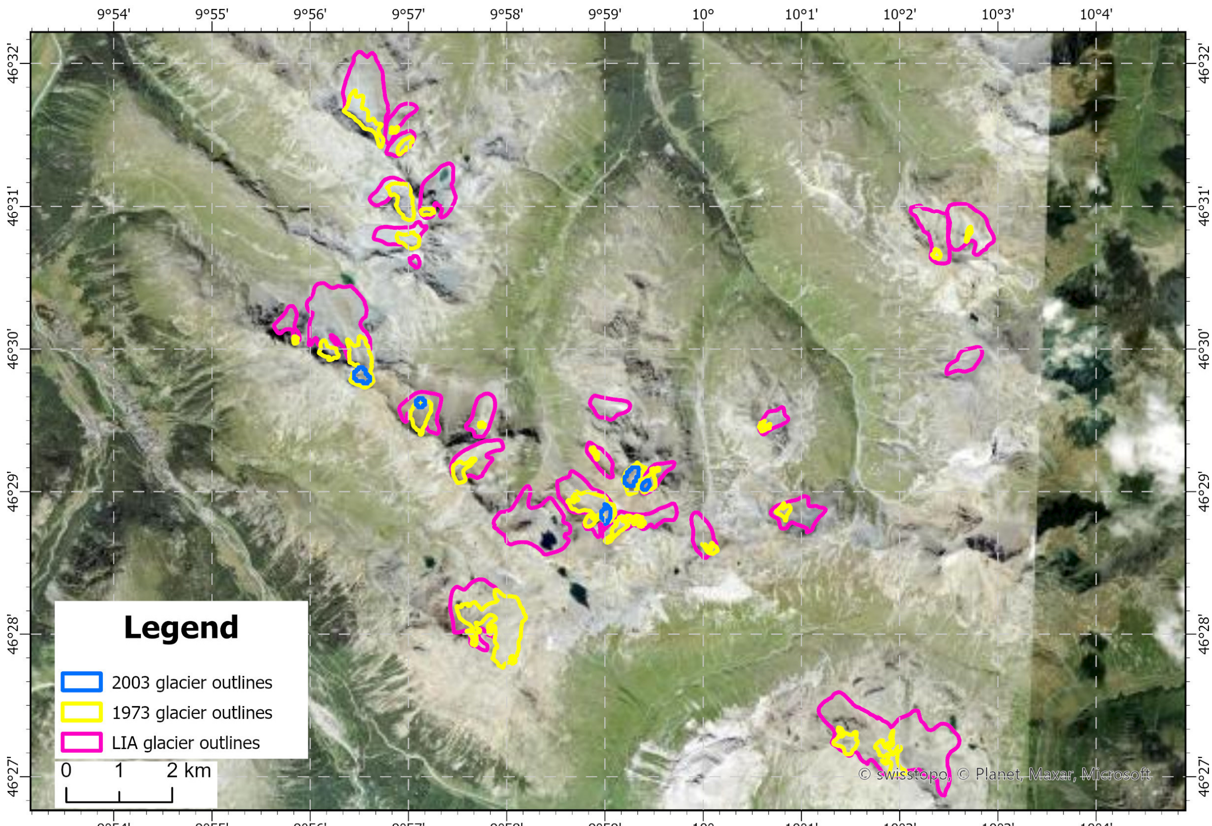

Figure S8: Examples of an already glacier-free (no glaciers in 2015) basin (Val Chamuera in Engadin, Switzerland). Background: ESRI, (2023b).

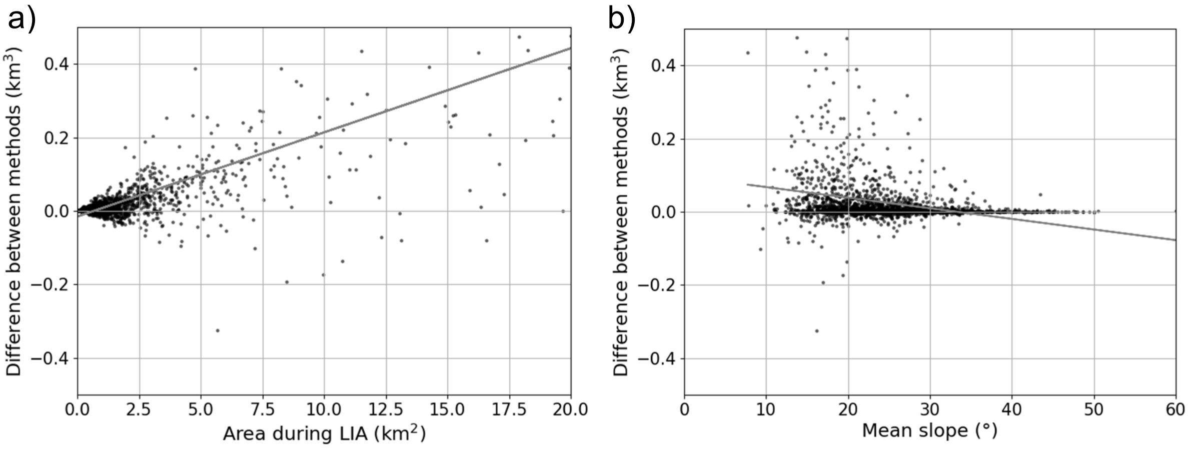

Figure S9: a) Difference in volume change (km^3) per glacier between the two methods (GIS-based and parameterisation scheme) against the initial area. b) The difference between the methods against the mean slope. Positive values indicate the calculated volume change in the GIS approach being larger.

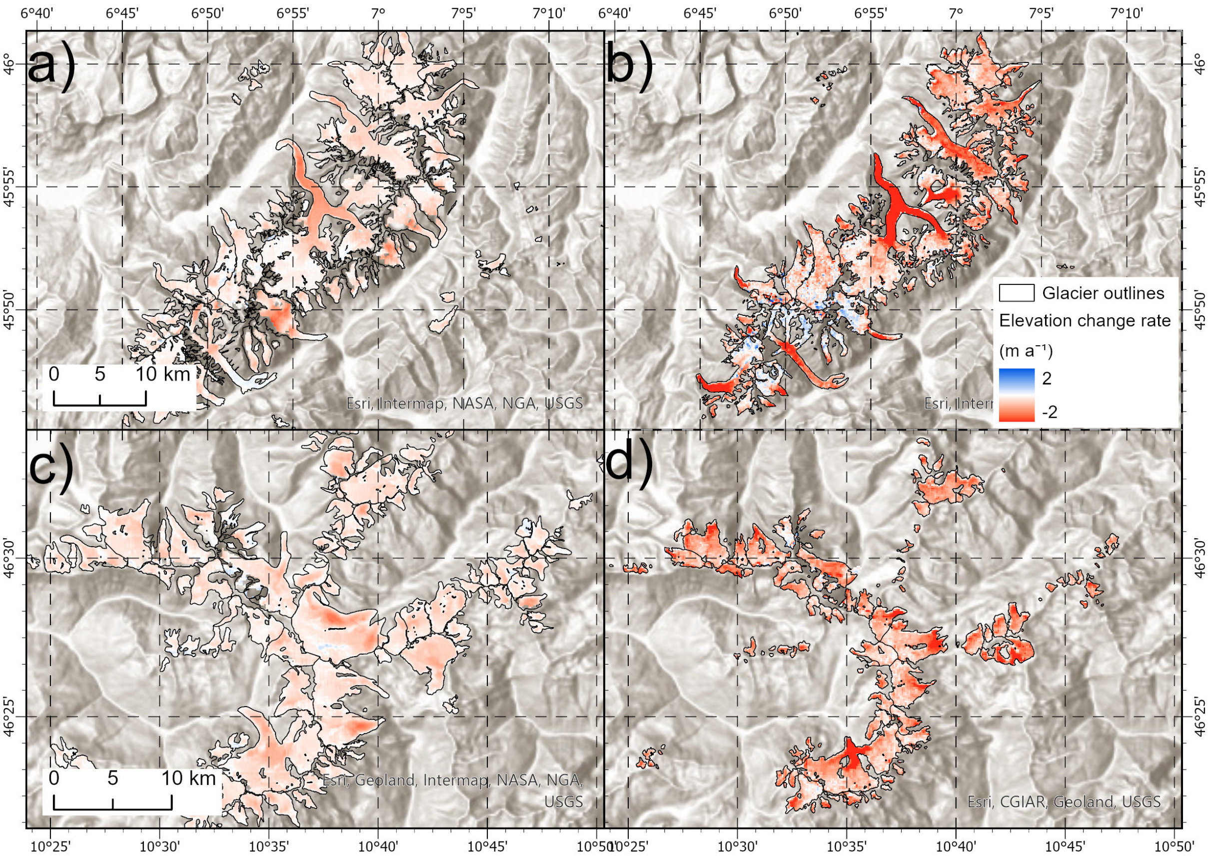

Figure S10: Examples of elevation change rates between the LIA and 2000 (P1) (a & c) and 2000-2014 (P2) after Hugonnet et al. (2021) (b & d) for the Mt. Blanc region (a & b) and the Ortles-Cevedale group (c & d) using the same colour legend for all panels. All background images: ESRI (2023a).

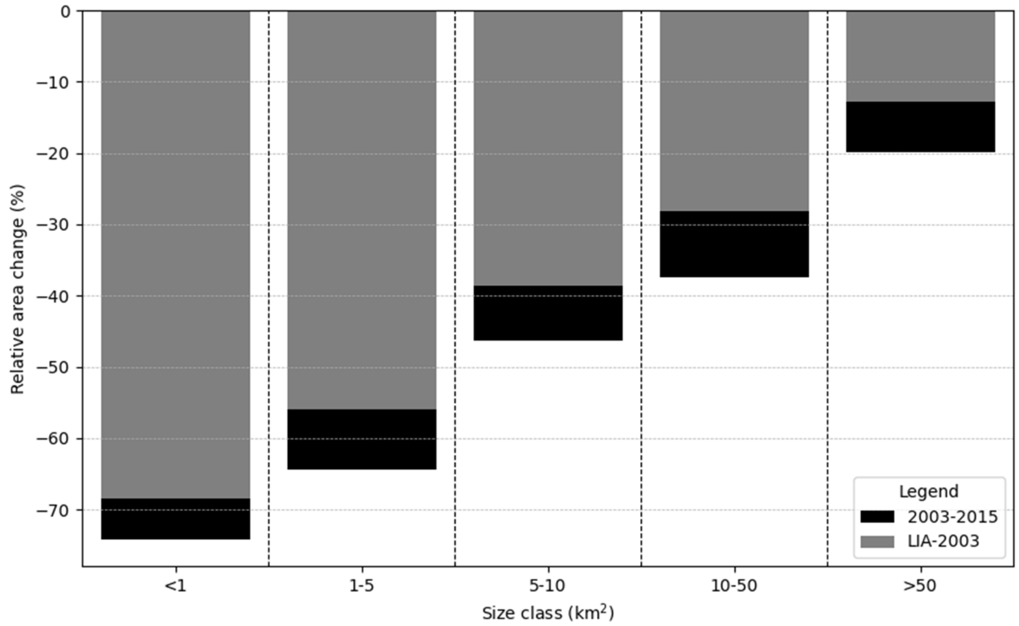

Figure S11: Relative glacier area changes per size class since the LIA.

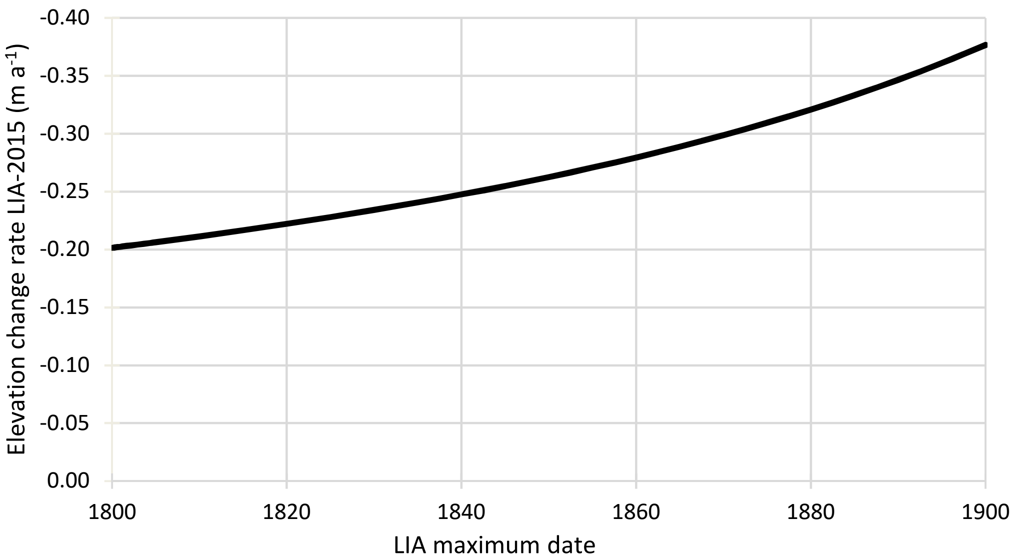

Figure S12: Effect of LIA starting date on elevation and volume change rates.

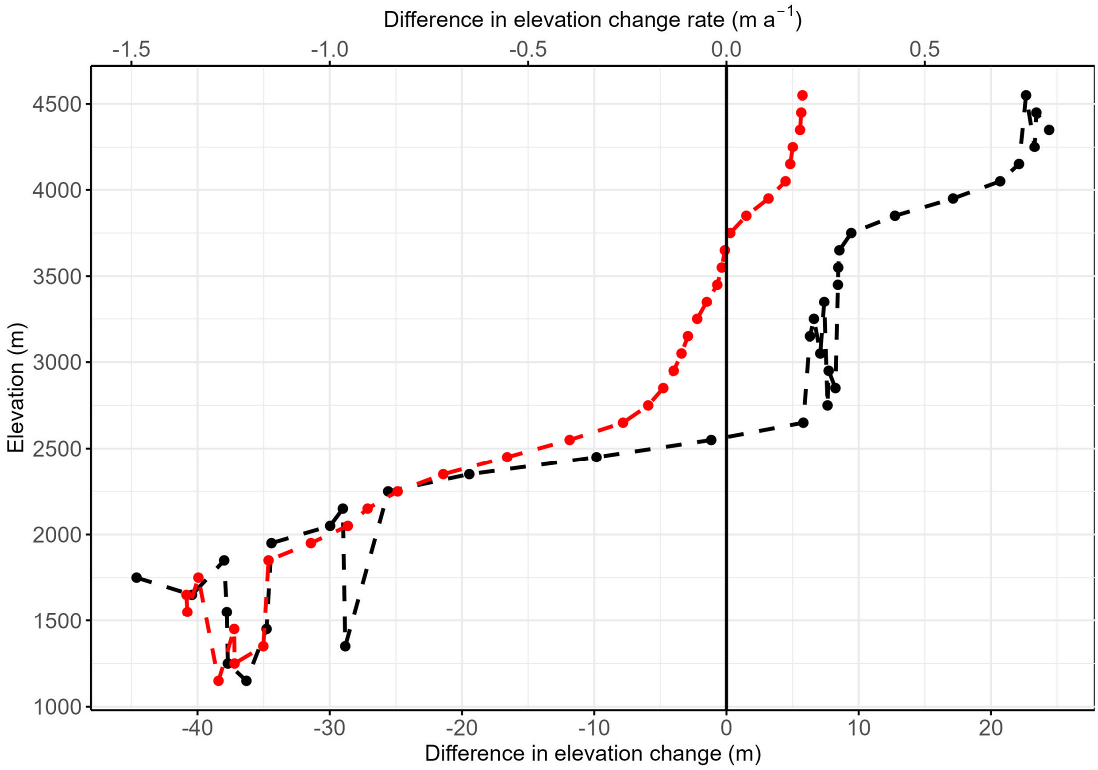

Figure S13: Elevation dependent differences between glacier elevation change values from this study to the dataset from Mannerfelt et al. (2022). In black the difference in elevation change and in red the difference in elevation change rate. Negative values indicate that the data from Mannerfelt et al. (2022) had higher elevation change (rate) values, the opposite for positive values.

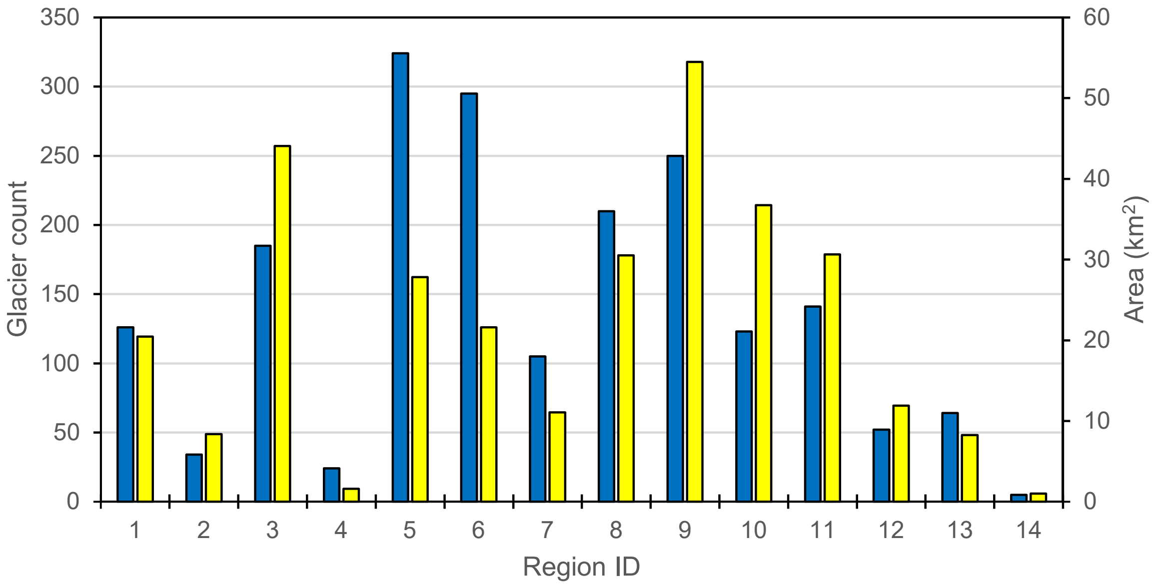

Figure S14: Number (blue, left y-axis) and area (yellow, right y-axis) of glacier LIA glaciers that have melted away completely by 2015.

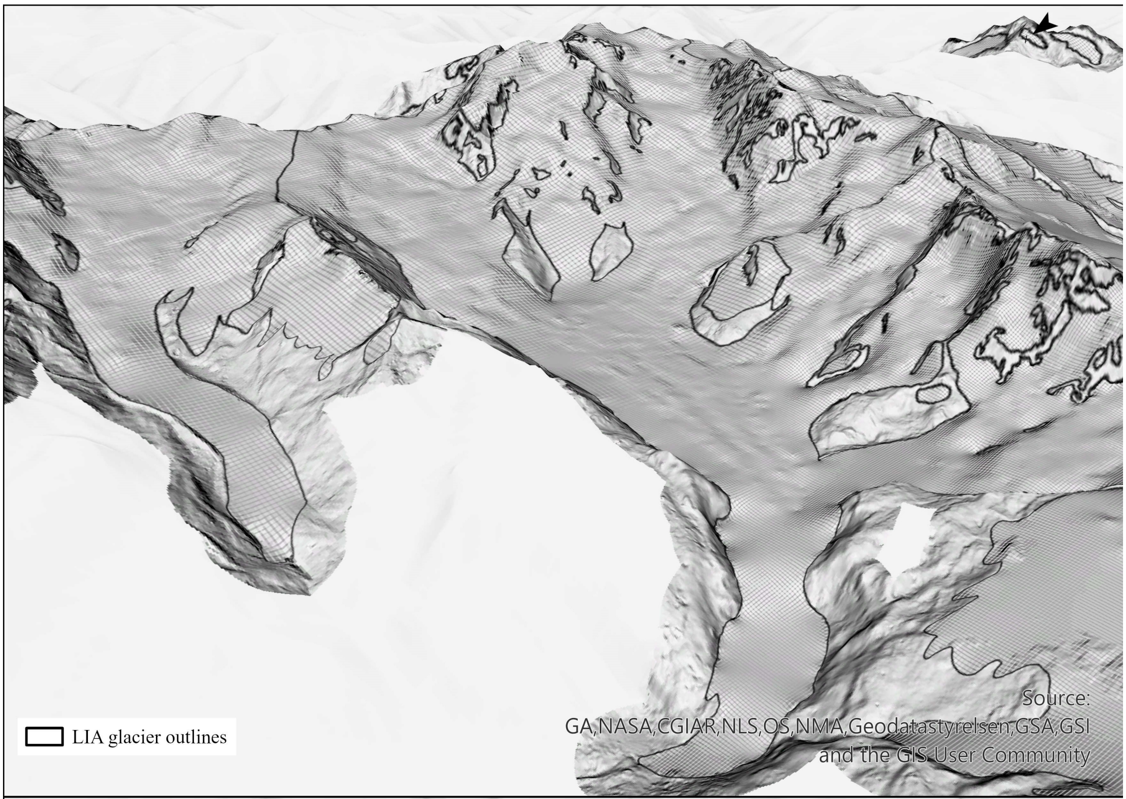

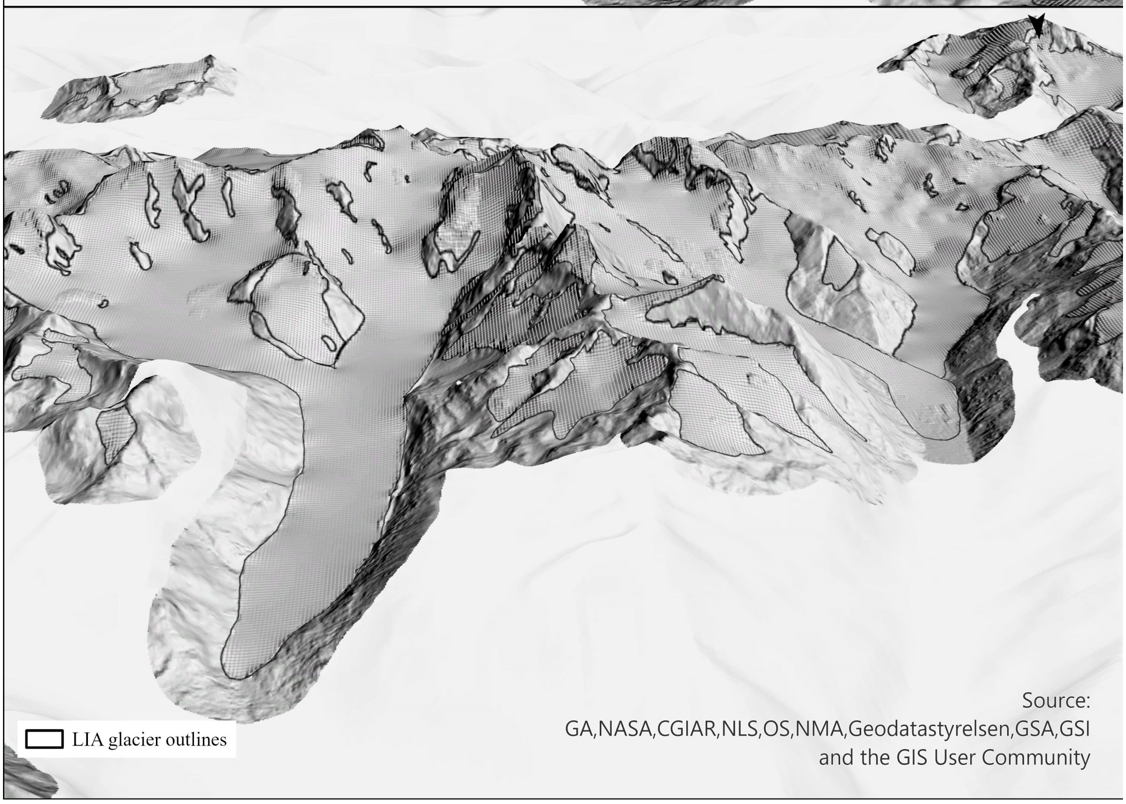

Figure S15: Hillshade of Monte Rosa and Bernina at the end of the LIA.

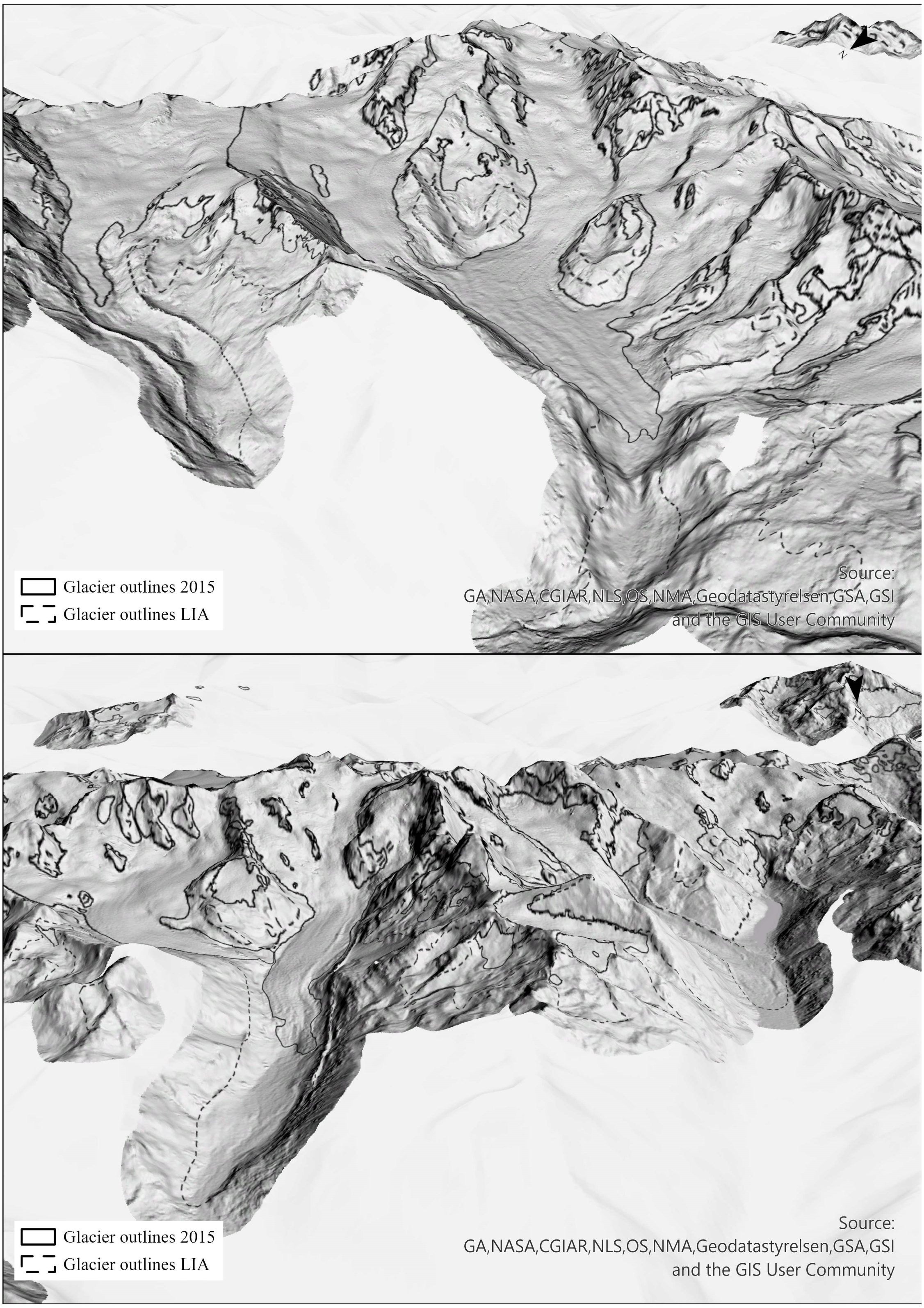

Figure S16: Hillshade of Monte Rosa and Bernina in 2015.

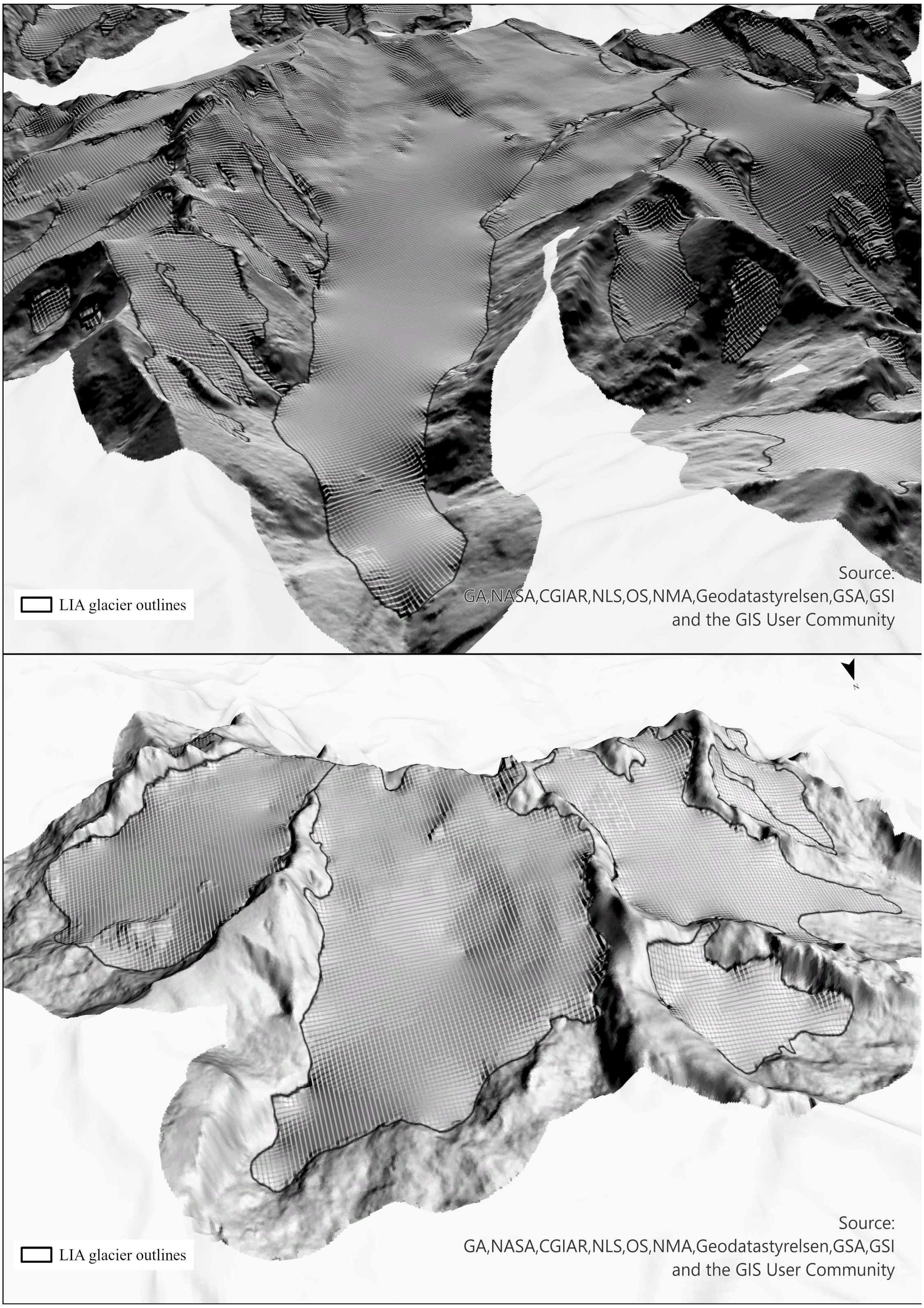

Figure S17: Hillshade of Pasterze and Dachstein at the end of the LIA.

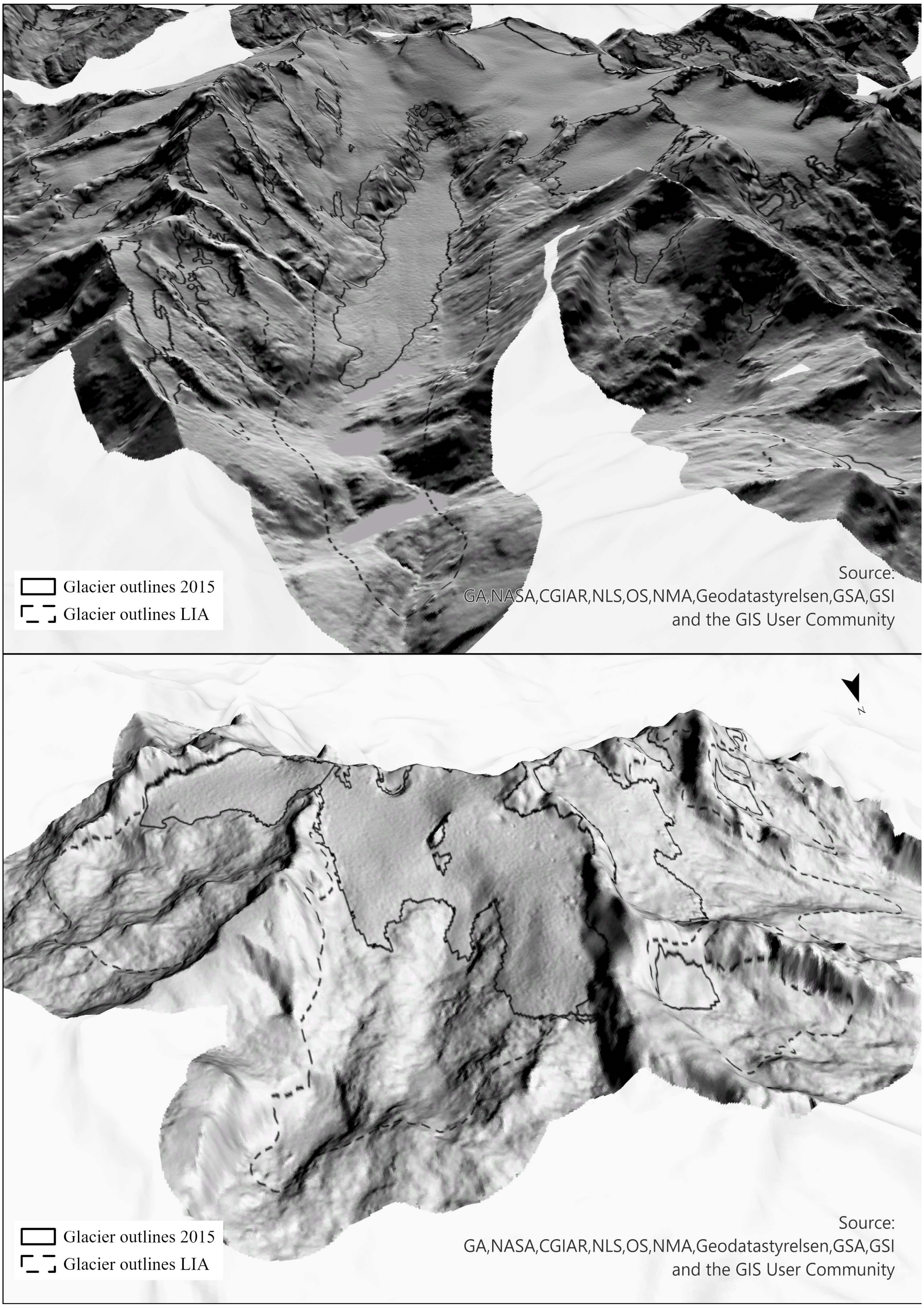

Figure S18: Hillshade of Pasterze and Dachstein in 2015.

S3 Uncertainty calculation

In the following, we describe the impact of the individual components on the volume uncertainty. The relative area uncertainty (ε_A/A) was taken from Reinthaler and Paul (2023), who determined the reproduction and interpretation uncertainties from multiple digitising experiments. They found a mean deviation of 1.9% with a standard deviation of ±5.05%. If the latter is taken as the relative uncertainty and applied to the sample of this study, the total LIA volume would be 280±14.1 km^3.

The uncertainty of the surface reconstruction ($\varepsilon_s/\mathrm{H}_{mean}$) was taken from Reinthaler and Paul (2024), who gave a vertical uncertainty of 4.6 m as the mean difference between the reconstructed LIA surface of the Bernese Alps and the reference DEM (Dufour Atlas). This change of mean glacier thickness would lead to a change in the total volume of 6.98% or 280±19.5 km^3.

The uncertainty values relating to the ice thickness (bedrock elevation) data ($\varepsilon_b/\mathrm{H}_{mean}$) were taken from the studies of the related datasets (see Table S6) and applied to our LIA dataset. As the area and surface uncertainty were neglected in these studies, their volume uncertainties are only due to thickness uncertainties. For glaciers in Austria, Helfricht et al. (2019) gave an uncertainty of 5% and for Switzerland, Grab et al. (2021) determined a value of 4.1%. For the remaining glaciers (France, Italy, Germany and Slovenia), the uncertainty was taken from Millan et al. (2022) who conservatively estimated it to be 30%. When considering the uncertainties from the three sources and calculate the proportional contribution to the LIA dataset from this study (Table S6), the resulting volume uncertainty is 12.7%, giving a total LIA volume of 280±36 km^3.

Table S6: Uncertainty calculation of the impact of the ice thickness dataset on the total volume.

Country	LIA volume (km^3)	Ice thickness dataset	Uncertainty value (%)	Lower bound LIA volume (km^3)	Upper bound LIA volume (km^3)
FR	33.64	(Millan et al., 2022)	30	23.55	43.73
CH	133.51	(Grab et al., 2021)	4.1	128.04	138.99
IT	57.65	(Millan et al., 2022)	30	40.35	74.94
AT	56.00	(Helfricht et al., 2019)	5	53.20	58.80
DE	0.13	(Millan et al., 2022)	30	0.09	0.17
SI	0.02		30	0.01	0.02
Total	279.6		12.7	245.3	361.6

The total relative volume uncertainty (ε_V/V) was calculated from the above individual uncertainties as $\varepsilon_V/V = \sqrt{(5.05^2 + 6.98^2 + 12.70^2)}$ resulting in 15.3% and a total LIA volume of 280±43 km^3.

On top of the upper bound of 322 km^3, an underestimation by 0.17 km^3 from glaciers without LIA equivalent has to be considered. The total area of these glaciers in RGI v7.0 is 12.1 km^2. With a relative change of 68.4% for glaciers smaller than 1 km^2 this gives a total LIA area of 38.37 km^2. The LIA volume was calculated by using the 2015 mean glacier thickness (h_F, calculated from the parameterisation scheme) and the LIA area. According to Parkes and Marzeion (2018), glaciers which completely melted away are responsible for 4.4 mm (lower bound) of sea-level rise compared to a total of 89.1 mm between 1901 and 2015. This 4.7% difference would add an additional 13.2 km^3 of lost glacier volume to our sample and together with the 0.17 km^3 for the glaciers without LIA extents results in an underestimation of 13.3 km^3. Taking all factors into account, the upper boundary for the total LIA volume would be 336 km^3. In Table S7 we summarize all uncertainty components and their influence on the LIA glacier volume.

Table S 7: Overview of the uncertainty components and their influence on the total LIA volume. Also, components of a possible underestimation and their influence on the upper bound of the LIA volume estimation.

Uncertainties	Area	Surface	Bed	Total	Underestimation not mapped glaciers	Underestimation glaciers already melted away	Total underestimation
Relative uncertainty (%)	5.05	6.98	12.70	15.35	0.06	4.71	4.77
Absolute uncertainty on LIA volume (km^3)	14.12	19.52	35.51	42.81	0.17	13.2	13.3
Lower bound (km^3)	265.51	260.11	244.12	236.82			
Upper bound (km^3)	293.75	299.16	315.14	322.44	322.61	335.60	335.77

For the uncertainty of glacier volume in 2016, we used the same relative uncertainty values as for the LIA volume. This approach provides a conservative estimate as it assumes that the relative uncertainties associated with glacier area, surface elevation and ice thickness are similar in the two time periods. While this may slightly overestimate the uncertainties for the more recent dataset(as glacier outlines and the DEMs used have better quality), it ensures consistency and avoids introducing additional complexity into the analysis.

For the uncertainty of the relative volume change between the LIA and 2016 ($\varepsilon_{\Delta V}/\Delta V$), we combined the relative uncertainties of the two volumes as follows:

$$\varepsilon_{\Delta V}/\Delta V = \sqrt{(\varepsilon_{LIA}/V_{LIA})^2 + (\varepsilon_{2016}/V_{2016})^2},$$

giving an uncertainty of the volume change estimate of 21.7%.

S4 Parameter calculations

1. Calculate length [$L0$] of each glacier: taken from centrelines using OGGM script (Maussion et al., 2019). Length of the ablation area [La]= $L0$/2
2. Calculate min and max elevation for each glacier: Taken from the Copernicus DEM (ESA, 2019)
3. Elevation range: $dH = H_{max} - H_{min}$
4. Calculate average slope: $a = \text{aretan}[\frac{dH}{Lo}]$
5. Mean basal shear stress: $\tau_f = 0.005 + 1.598 * dH - 0.435 * dH$
6. Average ice depth along the flowline: $h_f = \frac{\tau_f}{f\rho g \sin\alpha}$ where the shape factor f = 0.8; g is the gravitational acceleration 9.81 m s^{-2}; and p = the ice density (900 kg m^{-3})
7. Average thickness for a semi-elliptical profile: $h_F = (\frac{\pi}{4})h_f$
8. Volume: $V = A * h_F$; A being the glacier area
9. Temperature changes from ELA changes: $\delta T = \frac{\delta ELA}{\text{lr}}$ lr being the lapse rate

S5 Additional references

Colucci, R. R. and Žebre, M.: Late Holocene evolution of glaciers in the southeastern Alps, J Maps, 12, 289–299, https://doi.org/10.1080/17445647.2016.1203216, 2016.

ESA: Copernicus DEM EEA-10, https://doi.org/10.5270/ESA-c5d3d65, 2019.

ESRI: “Topographic” [basemap]. scale not given. “World Topographic Map,” 2023a.

ESRI: “World Imagery” [basemap]. scale not given. “World Imagery Vivid,” 2023b.

Fischer, A., Seiser, B., Stocker Waldhuber, M., Mitterer, C., and Abermann, J.: Tracing glacier changes in Austria from the Little Ice Age to the present using a lidar-based high-resolution glacier inventory in Austria, Cryosphere, 9, 753–766, https://doi.org/10.5194/tc-9-753-2015, 2015.

Gardent, M.: Inventaire et retrait des glaciers dans les Alpes françaises depuis la fin du Petit Age Glaciaire, Université de Savoie, 444 pp., 2014.

Grab, M., Mattea, E., Bauder, A., Huss, M., Rabenstein, L., Hodel, E., Linsbauer, A., Langhammer, L., Schmid, L., Church, G., Hellmann, S., Deleze, K., Schaer, P., Lathion, P., Farinotti, D., and Maurer, H.: Ice thickness distribution of all Swiss glaciers based on extended ground-penetrating radar data and glaciological modeling, Journal of Glaciology, 67, 1074–1092, https://doi.org/10.1017/jog.2021.55, 2021.

Groß, G.: Der Flächenverlust der Gletscher in Österreich 1850 – 1920 – 1969, Zeitschrift für Gletscherkunde und Glazialgeologie, 23, 131–141, 1987.

Helfricht, K., Huss, M., Fischer, A., and Otto, J. C.: Calibrated ice thickness estimate for all glaciers in Austria, Front Earth Sci (Lausanne), 7, 1–15, https://doi.org/10.3389/feart.2019.00068, 2019.

Hugonnet, R., McNabb, R., Berthier, E., Menounos, B., Nuth, C., Girod, L., Farinotti, D., Huss, M., Dussaillant, I., Brun, F., and Kääb, A.: Accelerated global glacier mass loss in the early twenty-first century, Nature, 592, 726–731, https://doi.org/10.1038/s41586-021-03436-z, 2021.

Knoll, C., Kerschner, H., Heller, A., and Rastner, P.: A GIS-based reconstruction of little ice age glacier maximum extents for South Tyrol, Italy, Transactions in GIS, 13, 449–463, https://doi.org/10.1111/j.1467-9671.2009.01173.x, 2009.

Lucchesi, S., Fioraso, G., Bertotto, S., and Chiarle, M.: Little Ice Age and contemporary glacier extent in the Western and South-Western Piedmont Alps (North-Western Italy), J Maps, 10, 409–423, https://doi.org/10.1080/17445647.2014.880226, 2014.

Maisch, M., Wipf, A., Denneler, B., Battaglia, J., and Benz, C.: Die Gletscher der Schweizer Alpen: Gletscherhochstand 1850, aktuelle Vergletscherung, Gletscherschwundszenarien, in: Schlussbericht NFP 31, second edition, Hochschulverlag ETH Zurich, Zurich, 373p, 2000.

Mannerfelt, E. S., Dehecq, A., Hugonnet, R., Hodel, E., Huss, M., Bauder, A., and Farinotti, D.: Halving of Swiss glacier volume since 1931 observed from terrestrial image photogrammetry, Cryosphere, 16, 3249–3268, https://doi.org/10.5194/tc-16-3249-2022, 2022.

Maussion, F., Butenko, A., Champollion, N., Dusch, M., Eis, J., Fourteau, K., Gregor, P., Jarosch, A. H., Landmann, J., Oesterle, F., Recinos, B., Rothenpieler, T., Vlug, A., Wild, C. T., and Marzeion, B.: The Open Global Glacier Model (OGGM) v1.1, Geosci. Model Dev., 12, 909–931, https://doi.org/10.5194/gmd-12-909-2019, 2019.

Millan, R., Mouginot, J., Rabatel, A., and Morlighem, M.: Ice velocity and thickness of the world's glaciers, Nat Geosci, 15, 124–129, https://doi.org/10.1038/s41561-021-00885-z, 2022.

Müller, F., Caflisch, T., and Müller, G.: Firn und Eis der Schweizer Alpen: Gletscherinventar, Geographisches Institut Publ. 57, Zurich, Eidgenössische Technische Hochschule, 1976.

Parkes, D. and Marzeion, B.: Twentieth-century contribution to sea-level rise from uncharted glaciers, Nature, 563, 551–554, https://doi.org/10.1038/s41586-018-0687-9, 2018.

Paul, F., Rastner, P., Azzoni, R. S., Diolaiuti, G., Fugazza, D., Bris, R. Le, Nemec, J., Rabatel, A., Ramusovic, M., Schwaizer, G., and Smiraglia, C.: Glacier shrinkage in the Alps continues unabated as revealed by a new glacier inventory from Sentinel-2, Earth Syst Sci Data, 12, 1805–1821, https://doi.org/10.5194/essd-12-1805-2020, 2020.

Reinthaler, J. and Paul, F.: Using a Web Map Service to map Little Ice Age glacier extents at regional scales, Ann Glaciol, 1–19, https://doi.org/https://doi.org/10.1017/ aog.2023.39, 2023.

Reinthaler, J. and Paul, F.: Assessment of methods for reconstructing Little Ice Age glacier surfaces on the examples of Novaya Zemlya and the Swiss Alps, Geomorphology, 461, https://doi.org/https://doi.org/10.1016/j.geomorph.2024.109321 Received, 2024.

RGI 7.0 Consortium: Randolph Glacier Inventory - A Dataset of Global Glacier Outlines, Version 7.0, https://doi.org/10.5067/f6jmovy5navz, 2023.

Scotti, R. and Brardinoni, F.: Evaluating millennial to contemporary time scales of glacier change in Val Viola, Central Italian Alps, Geografiska Annaler, Series A: Physical Geography, 100, 319–339, https://doi.org/10.1080/04353676.2018.1491312, 2018.

Sommer, C., Malz, P., Seehaus, T. C., Lippl, S., Zemp, M., and Braun, M. H.: Rapid glacier retreat and downwasting throughout the European Alps in the early 21st century, Nat Commun, 11, https://doi.org/10.1038/s41467-020-16818-0, 2020.

Vivian, R.: Les glacier des Alpes occidentales, Grenoble: Allier, 1975.

Zanoner, T., Carton, A., Seppi, R., Carturan, L., Baroni, C., Salvatore, M. C., and Zumiani, M.: Little Ice Age mapping as a tool for identifying hazard in the paraglacial environment: The case study of Trentino (Eastern Italian Alps), Geomorphology, 295, 551–562, https://doi.org/10.1016/j.geomorph.2017.08.014, 2017.